HHS Public Access

Author manuscript

Muscle Nerve. Author manuscript; available in PMC 2017 January 01.

Published in final edited form as:

Muscle Nerve. 2016 January ; 53(1): 84–90. doi:10.1002/mus.24675.

Age-related T_2 changes in hindlimb muscles of *mdx* mice

Ravneet S Vohra, PhD[1], **Sunita Mathur, PhD**[3], **Nathan D. Bryant, PhD**[2], **Sean C. Forbes, PhD**[1], **Krista Vandenborne, PhD**[1], and **Glenn A Walter, PhD**[2]

[1]Department of Physical Therapy, University of Florida, Gainesville, Florida, USA

[2]Department of Physiology and Functional Genomics, University of Florida, Box, 100274, Gainesville, Florida 32610-0274, USA

[3]Department of Physical Therapy, University of Toronto, 500 University Ave, Toronto ON Canada, M5G 1V7

Abstract

Introduction—Magnetic resonance imaging (MRI) was used to monitor changes in the transverse relaxation time constant (T_2) in lower hindlimb muscles of *mdx* mice at different ages.

Methods—Young (5 wks), adult (44 wks), old *mdx* (96 wks), and age-matched control mice were studied. Young *mdx* mice were imaged longitudinally, whereas adult and old *mdx* mice were imaged at a single time point.

Results—Mean muscle T_2 and percent of pixels with elevated T_2 were significantly different between *mdx* and control mice at all ages. In young *mdx* mice, mean muscle T_2 peaked at 7–8 weeks and declined at 9–11 weeks. In old *mdx* mice, mean muscle T_2 was decreased compared to young and adult, which could be attributed to fibrosis.

Conclusions—MRI captured longitudinal changes in skeletal muscle integrity of *mdx* mice. This information will be valuable for pre-clinical testing of potential therapeutic interventions for muscular dystrophy.

Keywords

magnetic resonance imaging; *mdx* mouse; Duchenne muscular dystrophy; muscle T_2; inflammation; fibrosis

Introduction

Duchenne muscular dystrophy (DMD) is an X-linked recessive neuromuscular disease with an incidence of 1 in 3,600 to 6,000 male births[1]. DMD is caused by a mutation in the *dystrophin* gene, which encodes for dystrophin, a 427 KDa cytoskeletal protein[2]. Dystrophin is hypothesized to participate in cytoskeletal organization, stability, and membrane

Please address correspondence to: G.A. Walter; glennw@ufl.edu.

Financial disclosure: The authors have no financial relationship with the manufacturers of any product or equipment discussed in this manuscript.

Conflict of interest: The authors of this manuscript declare that there is no conflict of interest.

integrity[3]. The *mdx* mouse, the most commonly used animal model of DMD, offers an economical way for pre-clincial testing of possible therapeutic interventions. *mdx* mice are similar to DMD patients in that they lack dystrophin and share some biochemical and histopathological features[4]. Despite the similarities, the phenotype of *mdx* mice is less severe than DMD patients. Skeletal muscles of *mdx* mice undergo repeated cycles of degeneration and regeneration even during adult life[5,6] whereas the regenerative capacity appears to be exhausted at an early age in humans with DMD. Many histological studies have confirmed that hindlimb muscles[7] and diaphragm[8] of *mdx* mice show progressive weakness and deterioration with age. Furthermore, the phenotype exhibited by old *mdx* mice more closely resembles changes observed in DMD boys (i.e increased fibrosis and fatty tissue deposition)[9].

Histological markers of muscle damage, such as Evans Blue dye[10,11] and Procion orange dye[12] have been used extensively to measure efficacy of restoring sarcolemmal integrity in pre-clinical trials. The major drawback of these *ex vivo* measurements is that they can be done only at the end point or when mice are sacrificed. In addition to developing effective therapeutic agents, there have been increasing efforts to develop non-invasive diagnostic biomarkers to understand the progression of disease and effects of therapy[13,14]. One method, magnetic resonance imaging (MRI), provides the ability to monitor disease progression non-invasively and may provide valuable information on understanding the progression of the disease in both animal models and humans.

Proton transverse relaxation time constant (T_2) is a quantitative MR measure used to detect changes in healthy and pathological muscle. Previous studies have used muscle T_2 to monitor muscle damage and repair in animal models of spinal cord injury[15], cast immobilization,[16] and muscular dystrophy[17–19]. Alterations in muscle T_2 have been attributed to muscle damage[20], edema[21,22], fatty tissue infiltration[23], and fibrosis[24]. In this study we utilized T_2 MRI to monitor the pathological changes in *mdx* mice lower hindlimb muscles with age. Furthermore, changes in muscle T_2 were compared to standard histological markers of muscle damage and fibrosis.

Methods

Animals

C57BL/10ScSn-DMD*mdx* (*mdx*; n=18) and C57BL/10ScSn (Ctrl; n=12) male mice were included in the study. *mdx* and Ctrl mice were obtained from Jackson laboratories (Bar Harbor, ME), and were thereafter maintained in-house. Animals were housed in an AAALAC approved facility with 12-hour light:dark cycle (72°F, 42% humidity) and free access to food and water. The University's Institutional Animal Care and Use Committee approved the experimental protocol.

Experimental protocol

Three age groups of *mdx* and age-matched Ctrl mice were studied: 1) young mice aged 5 wks, *mdx* (n=6) and Ctrl (n=4); 2) adult mice aged 44 wks, *mdx* (n=6) and Ctrl (n=4); and 3) old mice aged 96 wks, *mdx* (n=6) and Ctrl (n=4). Young Ctrl mice were imaged at a single

time point, whereas young *mdx* mice were imaged longitudinally at the following time points: 5, 6, 7, 8, 9, 10, 11, 13, 14, 17, 21, and 24 weeks of age. Adult and old *mdx* and age-matched Ctrl mice were imaged at single time points (44 and 96 weeks of age, respectively, see Figure 1).

Magnetic Resonance Imaging

MRI was performed in a 4.7 T horizontal bore magnet (Bruker Avance). The animals were anesthetized using an oxygen and isoflurane mixture (3% isoflurane) and maintained under 0.5–1% isoflurane for the duration of the MR procedure. Respiratory rate of the mouse was monitored throughout the scan. The lower hindlimbs of the mouse were inserted up to the knee into a 2.0 cm internal diameter, custom-built solenoid ^{1}H coil (200 MHz). T_2-weighted MR images were acquired with the following parameters: multiple slice, single spin-echo images were acquired with repetition time (TR) =2,000ms, echo time (TE)=14ms and 40ms, FOV 10–20mm, slice thickness 0.5–1mm, acquisition matrix = 128 × 256, and 2 signal averages[10]. Diffusion weighting was fixed at both TEs (diffusion weighting 3 mm^2/s at both 14 and 40 ms). Hahn spin echoes were implemented to avoid the contribution of stimulated echoes in the T_2 measurement[10,25]. The T_2 decay was fit to a single exponential decay curve[10]. Based on our previous work, we find that calculating T_2 from 2 echoes is sufficient to distinguish between healthy and damaged muscle. This method also has high between-day reproducibility in control mice (n=10, coefficient of variation of 2.3 % for anterior and 3.4% for posterior compartments). Signal-to-noise ratios were 25:1 at TE = 14 ms and 9:1 at TE = 40 ms.

Muscle T_2 Analysis from MRI

Muscle T_2 values of the middle 6–8 slices from anterior and posterior compartments of hindlimbs (Figure 2) were computed and analyzed from T_2 maps created from 2 echo times (TEs: 14 and 40 ms) using in-house software as described previously[16]. This was done in order to improve the coverage and to increase the reliability. T_2 was calculated using the following equation: $T_2 = (26\ ms)/\ln(SI_{14}/SI_{40})$, where SI 14 and SI 40 are the pixel intensities at TE of 14 ms and 40 ms, respectively[26]. The percent of muscle damage detected by MRI was defined as the percentage of pixels in a region of interest (ROI) which had T_2 values over 2 standard deviations above the mean muscle T_2 found in control mice (> 29ms) up to a maximum value of 100 ms.

Histology

We performed a qualitative histological evaluation of hind limb muscles in 24 weeks and 96-week old *mdx* (n = 3) and Ctrl (n = 3) mice. Different lower limb muscles, including tibialis anterior (TA), extensor digitorum longus (EDL), gastrocnemius (Gastr), and soleus (SOL) were dissected carefully from the hindlimbs, fixed at resting length, frozen immediately in melting isopentane precooled in liquid nitrogen, and then stored at −80°C for further analysis. Ten-micron slices of the samples were taken from the mid-belly region, then stained with hematoxylin and eosin (H&E) and Trichrome. H&E stained cross sections were evaluated visually for morphological characteristics, such as the presence of inflammatory infiltrates and centrally nucleated fibers (CNFs). CNFs were quantified in *mdx*

and Ctrl mice. The samples were also stained with Masson trichrome to determine collagen tissue deposition (i.e. fibrotic area). Percent CNFs and fibrotic area was quantified using ImageJ software (NIH, 1.47v), and the fibrosis index was defined as fibrotic area divided by total area × 100[27].

Statistical Analysis

All statistical analysis was performed using SPSS for Mac (version 20.0). The coefficient of variance was computed to examine the variability between repeated measures in Ctrl mice. Results were expressed as mean ± standard deviation (SD) unless specified as mean ± standard error of the mean (SEM). Research hypotheses were tested at an alpha level of 0.05. One-way analysis of variance (ANOVA) for repeated measurements was performed to monitor the changes in hindlimb muscles of young *mdx* mice. Independent-sample *t*-tests were used to make comparisons between control and *mdx* groups at each time point (α=0.05, adjusted for multiple comparisons using a modified Bonferonni correction).

Results

T_2 variability

MR T_2 values were measured in Ctrl mice and were found to be highly reproducible. The average day-to-day reliability (CV) for the anterior compartment was 2.3% (25^{th} percentile, 0.65%; 75^{th} percentile, 3.8%), and for the posterior compartment it was 3.4%. (25^{th} percentile, 2.3%; 75^{th} percentile 3.9%).

Comparisons among age groups of *mdx* mice and controls

Mean muscle T_2 in the anterior compartments of young (5 – 24 weeks), adult (44 weeks), and old *mdx* mice (96 weeks) were significantly higher than age-matched control mice (Figure 3). However, in the posterior compartment, significant differences were observed only in the young and adult groups compared to controls. Old *mdx* mice showed lower T_2 compared to young and adult *mdx* mice (Figure 3).

The percentage of pixels with elevated T_2 in *mdx* mice, both in the anterior and posterior compartments were significantly different from age-matched control mice (Figure 4). In addition, the percentage of pixels with elevated T_2 in young *mdx* mice was significantly higher than in adult and old *mdx* mice.

T_2 changes in hindlimb muscles of young *mdx* mice

Young *mdx* mice presented with asynchronous, cyclical changes in both anterior and posterior compartments with age (Figure 5). In the anterior compartment, there was an increase in the mean muscle T_2 from 5 to 7 weeks, followed by a significant decrease at 10 weeks. Muscle T_2 values were higher at 11, 13, 17, and 21 weeks as compared to the 10-week time point (Figure 5A). The number of pixels with elevated T_2 in the anterior compartment was 3-fold higher at the 7-week time point than the 5-week time point and remained elevated at the 8-week time point. Thereafter, the percentage of pixels with elevated T_2 significantly decreased at 9 weeks and remained below 4% until 11 weeks. The

percent pixels with elevated T_2 values increased at the 13-week time point, thereafter dropping down at 17, 21, and 24-weeks (Figure 5B).

Similar to the anterior compartment, the T_2 values in the posterior compartment showed cyclical changes. Mean muscle T_2 values of the posterior compartment at 8 weeks were significantly higher than at 10 weeks. Moreover, T_2 values at 10 weeks were reduced as compared to 5, 7, 11, 13, 17, and 21 weeks (Figure 5C). Variation in the percent pixels with elevated T_2 showed a similar cyclical pattern. There was a 2-fold increase in percent pixels with elevated T_2 from 5 to 6 weeks. This increase continued at 7 and 8 weeks. Following the 8-week time point, there was a significant decrease in percent pixels with elevated T_2 at 9 weeks. It remained less than 7% until 11 weeks and thereafter increasing at the 13-week time point. Furthermore, following 13 weeks, the percent pixels with elevated T_2 dropped to 6% at 17 and 18 weeks, respectively and increased at 21 weeks. However, at 24 weeks there was a decline in percent pixels with elevated T_2 (Figure 5D).

Histological analyses

Histological analysis of anterior (TA and EDL) and posterior hindlimb muscles (Gastr and SOL) of *mdx* mice showed a significant increase in number of CNFs compared to age-matched controls (Figure 6A). In addition, Masson trichrome staining of hindlimb muscles revealed greater fibrotic tissue accumulation in *mdx* mice at 96 weeks of age than at younger ages and controls (Supplementary Material, Figure S1). Old *mdx* muscles showed approximately 2-fold higher percentage of fibrotic area than adult *mdx* muscles (Figure 6B).

Discussion

These results show that T_2 is highest in young mice followed by asynchronous, cyclical alterations in muscle T_2 up to at least 6 months of age. Furthermore, we observed a decrease in percent pixels with elevated T_2, indicative of less muscle edema, damage, and inflammation, in adult and old *mdx* mice than in young *mdx* mice. Similar findings have been reported by Pratt et al[28] in a case study of an *mdx* mouse using T_2-weighted images. In this study we extend those findings and compare quantitative T_2 MR measurements in a group of mice with histological measurements.

mdx versus Controls

Muscle T_2 was higher in hindlimb muscles of *mdx* mice than in controls in all age groups. Elevated muscle T_2 has been reported in canine models of muscular dystrophy and in children with DMD[29,30]. Although the exact mechanism for this T_2 change is not completely understood, T_2 changes have been attributed to accumulation of fatty tissue[30], edematous tissue[22], and fibrotic tissue[24]. Previous studies have demonstrated shifts in muscle T_2 following muscle damage and regeneration in rats as well as in *mdx* mice[10,31,32]. A study by Cabello et al[32] observed changes in signal intensity on T_2-weighted images after inducing inflammatory processes using *Candida albicans* and confirming MR alterations by histological measurements. Similar studies have been conducted by Does et al[22] using λ-carrageenan inducing edema in rat muscles. Furthermore, Mcintosh et al[31] observed foci of

high signal intensity in *mdx* muscles that corresponded to dystrophic lesions in histological sections.

Changes in *mdx* muscle T_2 over lifespan

Despite the absence of dystrophin protein, *mdx* mice show minimal functional signs of dystrophic pathology during the majority of their lifespan. However, the *mdx* mouse model has been shown to display signs of pathology during early and late stages of life. The disease progression in *mdx* mice has been generally divided into 3 stages: young, adult, and old age.

Young

Muscles of young *mdx* mice have been reported to undergo cycles of degeneration/regeneration[33,34]. Although the cause of these cycles remains elusive, it has been suggested that increased degeneration may occur due to increased exploratory behavior and locomotor activity of young mice[4]. Correspondingly, in this study, T_2 in young *mdx* mice was significantly elevated as compared to old *mdx* mice. Furthermore, we found that there was more variation in mean muscle T_2 in young *mdx* mice than in older mice. Although the factors contributing to elevated T_2 are not well established, T_2 has also been correlated with the size of the extracellular fluid in denervated muscle[35]. Additionally, T_2 has also been shown to be sensitive to fiber type and fiber size change[36,37]. In this study we observed that *mdx* mice at 24 weeks of age had increased extravascular space as compared to age-matched controls as well as an increased number of fibers with central nuclei.

In young *mdx* mice, we found that mean muscle T_2 is elevated between 5–8 weeks and peaks at 7–8 weeks of age. Furthermore, it has been reported that muscle degeneration and regeneration in *mdx* mice becomes more pronounced between 3–8 weeks of age, decreases significantly thereafter, and is believed to continue at a lower rate after this period[38–40]. For example, the tibialis anterior muscle has been shown to demonstrate signs of necrosis from 3 weeks after birth[41,42]. Furthermore, Passaquin et al observed greater necrosis in the SOL than the EDL at 3 weeks with greater muscle damage in SOL (~86%) than in EDL (~36%) at about 5 weeks of age[43]. On the other hand, satellite cell replication has been reported to peak between weeks 4 and 8 and continues at a slower pace until at least 44 weeks of age[40]. The reason for the acute onset of pathological changes and cyclical degeneration and regeneration processes at this age is still unresolved. It has been postulated to be due to: 1) an increase of in-cage locomotor activity; and 2) downregulation of various genes, including utrophin[44]. In addition, Yokota et al [45] observed an increase in CNFs at 10 weeks of age, which correlated well with the increase in revertant fibers. Similarly, we observed that muscle T_2 and % pixels with elevated T_2 starts increasing from 5 weeks and continue to increase until 7–8 weeks of age. Thereafter, both parameters decreased significantly at 10 weeks of age. After the initial bout, hindlimb muscles displayed age-dependent cyclical alterations, most prominent until 24 weeks of age.

Adult

During the adult lifespan, muscles of adult *mdx* mice, despite being bigger and heavier than control mice, have reduced specific force. Skeletal muscles from *mdx* mice show low levels of necrotic and regenerated myofibers[4]. Similarly, we observed the presence of central

nuclei in young as well as adult *mdx* muscles. Furthermore, it has been reported that skeletal muscles of adult *mdx* mice do not show extensive fibrosis, except of the diaphragm[8]. The extent of involvement of different muscle groups varies and may be related to position or use of a muscle group in the body[20,46,47].

Old age

Older *mdx* mice show a more involved progressive dystrophic phenotype. Extensive fibrosis has been reported in skeletal muscles of old *mdx* mice[48,49]. Furthermore, T_2 has been shown to decrease with accumulation of fibrous connective tissue in old *mdx* mice[24]. Similarly, we observed a lower mean muscle T_2 in 96-week-old *mdx* mice compared to young *mdx* mice. The decrease in muscle T_2 may be attributed to accumulation of fibrotic tissue in muscles of old *mdx* mice as shown by an increase in collagenous tissue deposition. Previous studies have shown a significant correlation between T_2 and histological measurements of fibrosis in the diabetic heart[50]. Furthermore, MRI studies have established a correlation between shortened T_2 values with increasing degree of fibrosis[51,52].

It is important to consider the limitations of this study. First, the experiment may have benefited from performing analysis on the individual muscles, but we were not able to do this due to lack of resolution. Improvements would include analyzing individual muscles in anterior and posterior compartments. Second, T_2 in muscle has been reported to be multicomponent when using highly sampled echo trains[22,53–56]. In our analysis we used mono-exponential analysis based on the signal decay between 2 echo times. This dual-echo approach has been used previously[10,20,57] but has limitations due to an inability to resolve multiple components and poor performance at low SNR values. Conversely, using multi-exponential analysis it might have been possible to differentiate between fibrosis, muscle damage, and inflammation[22]. However, obtaining images at multiple TEs during *in vivo* experiments without the impact of simulated echoes on the primary echo decay can prove quite challenging.

In summary, our findings suggest that: 1) the age of *mdx* mice is important when assessing response to different therapeutic strategies; and 2) MR T_2 is a sensitive biomarker that can be used to monitor age-related changes in skeletal muscles of *mdx* mice.

Supplementary Material

Refer to Web version on PubMed Central for supplementary material.

Acknowledgments

The authors would like to thank Sean Germain for assistance with acquiring MR images. The study was supported by Muscular Dystrophy Association (MDA 4176), the National High Magnetic Field Lab (NHMFL), The Senator Paul D. Wellstone Muscular Dystrophy Cooperative Research Center (U54AR052646), Department of Defense (MD 110050), and the National Institutes of Health (R01HL78670).

Abbreviations

ANOVA analysis of variance

DMD	Duchenne muscular dystrophy
FOV	field of view
Gastr	gastrocnemius
MRI	magnetic resonance imaging
ROI	region of interest
SOL	soleus
T_2	muscle transverse relaxation time
TA	tibilais anterior
TE	echo time
TR	repetition time

References

1. Bushby K, Finkel R, Birnkrant DJ, Case LE, Clemens PR, Cripe L, Kaul A, Kinnett K, McDonald C, Pandya S, Poysky J, Shapiro F, Tomezsko J, Constantin C. Group DMDCCW. Diagnosis and management of Duchenne muscular dystrophy, part 1: diagnosis, and pharmacological and psychosocial management. Lancet neurology. 2010; 9(1):77–93. [PubMed: 19945913]
2. Hoffman EP, Brown RH Jr, Kunkel LM. Dystrophin: the protein product of the Duchenne muscular dystrophy locus. Cell. 1987; 51(6):919–928. [PubMed: 3319190]
3. Ervasti JM, Campbell KP. Membrane organization of the dystrophin-glycoprotein complex. Cell. 1991; 66(6):1121–1131. [PubMed: 1913804]
4. Grounds MD, Radley HG, Lynch GS, Nagaraju K, De Luca A. Towards developing standard operating procedures for pre-clinical testing in the mdx mouse model of Duchenne muscular dystrophy. Neurobiology of disease. 2008; 31(1):1–19. [PubMed: 18499465]
5. Anderson JE, Bressler BH, Ovalle WK. Functional regeneration in the hindlimb skeletal muscle of the mdx mouse. Journal of muscle research and cell motility. 1988; 9(6):499–515. [PubMed: 3209690]
6. Dangain J, Vrbova G. Muscle development in mdx mutant mice. Muscle Nerve. 1984; 7(9):700–704. [PubMed: 6543918]
7. Pastoret C, Sebille A. mdx mice show progressive weakness and muscle deterioration with age. J Neurol Sci. 1995; 129(2):97–105. [PubMed: 7608742]
8. Stedman HH, Sweeney HL, Shrager JB, Maguire HC, Panettieri RA, Petrof B, Narusawa M, Leferovich JM, Sladky JT, Kelly AM. The mdx mouse diaphragm reproduces the degenerative changes of Duchenne muscular dystrophy. Nature. 1991; 352(6335):536–539. [PubMed: 1865908]
9. Desguerre I, Mayer M, Leturcq F, Barbet JP, Gherardi RK, Christov C. Endomysial fibrosis in Duchenne muscular dystrophy: a marker of poor outcome associated with macrophage alternative activation. Journal of neuropathology and experimental neurology. 2009; 68(7):762–773. [PubMed: 19535995]
10. Frimel TN, Walter GA, Gibbs JD, Gaidosh GS, Vandenborne K. Noninvasive monitoring of muscle damage during reloading following limb disuse. Muscle Nerve. 2005; 32(5):605–612. [PubMed: 16003743]
11. Hamer PW, McGeachie JM, Davies MJ, Grounds MD. Evans Blue Dye as an in vivo marker of myofibre damage: optimising parameters for detecting initial myofibre membrane permeability. Journal of anatomy. 2002; 200(Pt 1):69–79. [PubMed: 11837252]
12. Consolino CM, Brooks SV. Susceptibility to sarcomere injury induced by single stretches of maximally activated muscles of mdx mice. Journal of applied physiology (Bethesda, Md: 1985). 2004; 96(2):633–638.

13. Heckmatt JZ, Dubowitz V. Detecting the Duchenne carrier by ultrasound and computerized tomography. Lancet. 1983; 2(8363):1364. [PubMed: 6139695]
14. Heckmatt JZ, Dubowitz V, Leeman S. Detection of pathological change in dystrophic muscle with B-scan ultrasound imaging. Lancet. 1980; 1(8183):1389–1390. [PubMed: 6104175]
15. Liu M, Bose P, Walter GA, Thompson FJ, Vandenborne K. A longitudinal study of skeletal muscle following spinal cord injury and locomotor training. Spinal cord. 2008; 46(7):488–493. [PubMed: 18283294]
16. Frimel TN, Kapadia F, Gaidosh GS, Li Y, Walter GA, Vandenborne K. A model of muscle atrophy using cast immobilization in mice. Muscle Nerve. 2005; 32(5):672–674. [PubMed: 16025524]
17. Dunn JF, Zaim-Wadghiri Y. Quantitative magnetic resonance imaging of the mdx mouse model of Duchenne muscular dystrophy. Muscle Nerve. 1999; 22(10):1367–1371. [PubMed: 10487902]
18. Kobayashi YM, Rader EP, Crawford RW, Iyengar NK, Thedens DR, Faulkner JA, Parikh SV, Weiss RM, Chamberlain JS, Moore SA, Campbell KP. Sarcolemma-localized nNOS is required to maintain activity after mild exercise. Nature. 2008; 456(7221):511–515. [PubMed: 18953332]
19. Walter G, Cordier L, Bloy D, Sweeney HL. Noninvasive monitoring of gene correction in dystrophic muscle. Magnetic resonance in medicine: official journal of the Society of Magnetic Resonance in Medicine/Society of Magnetic Resonance in Medicine. 2005; 54(6):1369–1376.
20. Mathur S, Vohra RS, Germain SA, Forbes S, Bryant ND, Vandenborne K, Walter GA. Changes in muscle T2 and tissue damage after downhill running in mdx mice. Muscle Nerve. 2011; 43(6): 878–886. [PubMed: 21488051]
21. Bryant ND, Li K, Does MD, Barnes S, Gochberg DF, Yankeelov TE, Park JH, Damon BM. Multi-parametric MRI characterization of inflammation in murine skeletal muscle. NMR in biomedicine. 2014
22. Fan RH, Does MD. Compartmental relaxation and diffusion tensor imaging measurements in vivo in lambda-carrageenan-induced edema in rat skeletal muscle. NMR in biomedicine. 2008; 21(6): 566–573. [PubMed: 18041804]
23. Elder CP, Apple DF, Bickel CS, Meyer RA, Dudley GA. Intramuscular fat and glucose tolerance after spinal cord injury--a cross-sectional study. Spinal cord. 2004; 42(12):711–716. [PubMed: 15303112]
24. Bo Li Z, Zhang J, Wagner KR. Inhibition of myostatin reverses muscle fibrosis through apoptosis. Journal of cell science. 2012; 125(Pt 17):3957–3965. [PubMed: 22685331]
25. Liu M, Bose P, Walter GA, Anderson DK, Thompson FJ, Vandenborne K. Changes in muscle T2 relaxation properties following spinal cord injury and locomotor training. European journal of applied physiology. 2006; 97(3):355–361. [PubMed: 16770473]
26. Prior BM, Ploutz-Snyder LL, Cooper TG, Meyer RA. Fiber type and metabolic dependence of T2 increases in stimulated rat muscles. Journal of applied physiology (Bethesda, Md: 1985). 2001; 90(2):615–623.
27. van Putten M, de Winter C, van Roon-Mom W, van Ommen GJ, t Hoen PA, Aartsma-Rus A. A 3 months mild functional test regime does not affect disease parameters in young mdx mice. Neuromuscular disorders: NMD. 2010; 20(4):273–280. [PubMed: 20307983]
28. Pratt SJ, Xu S, Mullins RJ, Lovering RM. Temporal changes in magnetic resonance imaging in the mdx mouse. BMC research notes. 2013; 6(1):262. [PubMed: 23837666]
29. Arpan I, Forbes SC, Lott DJ, Senesac CR, Daniels MJ, Triplett WT, Deol JK, Sweeney HL, Walter GA, Vandenborne K. T(2) mapping provides multiple approaches for the characterization of muscle involvement in neuromuscular diseases: a cross-sectional study of lower leg muscles in 5–15-year-old boys with Duchenne muscular dystrophy. NMR in biomedicine. 2013; 26(3):320–328. [PubMed: 23044995]
30. Kim HK, Laor T, Horn PS, Racadio JM, Wong B, Dardzinski BJ. T2 mapping in Duchenne muscular dystrophy: distribution of disease activity and correlation with clinical assessments. Radiology. 2010; 255(3):899–908. [PubMed: 20501727]
31. McIntosh LM, Baker RE, Anderson JE. Magnetic resonance imaging of regenerating and dystrophic mouse muscle. Biochemistry and cell biology = Biochimie et biologie cellulaire. 1998; 76(2–3):532–541. [PubMed: 9923723]

32. Ruiz-Cabello J, Carrero-Gonzalez B, Aviles P, Santisteban C, Mendez RJ, Ferreiros J, Malpica N, Santos A, Gargallo-Viola D, Regadera J. Magnetic resonance imaging in the evaluation of inflammatory lesions in muscular and soft tissues: an experimental infection model induced by Candida albicans. Magnetic resonance imaging. 1999; 17(9):1327–1334. [PubMed: 10576718]
33. DiMario JX, Uzman A, Strohman RC. Fiber regeneration is not persistent in dystrophic (MDX) mouse skeletal muscle. Dev Biol. 1991; 148(1):314–321. [PubMed: 1936568]
34. Pastoret C, Sebille A. Age-related differences in regeneration of dystrophic (mdx) and normal muscle in the mouse. Muscle Nerve. 1995; 18(10):1147–1154. [PubMed: 7659109]
35. Polak JF, Jolesz FA, Adams DF. Magnetic resonance imaging of skeletal muscle. Prolongation of T1 and T2 subsequent to denervation Investigative radiology. 1988; 23(5):365–369. [PubMed: 3384617]
36. Bonny JM, Zanca M, Boespflug-Tanguy O, Dedieu V, Joandel S, Renou JP. Characterization in vivo of muscle fiber types by magnetic resonance imaging. Magnetic resonance imaging. 1998; 16(2):167–173. [PubMed: 9508273]
37. English AE, Joy ML, Henkelman RM. Pulsed NMR relaxometry of striated muscle fibers. Magnetic resonance in medicine: official journal of the Society of Magnetic Resonance in Medicine/Society of Magnetic Resonance in Medicine. 1991; 21(2):264–281.
38. Anderson JE, Kao L, Bressler BH, Gruenstein E. Analysis of dystrophin in fast- and slow-twitch skeletal muscles from mdx and dy2J mice at different ages. Muscle Nerve. 1990; 13(1):6–11. [PubMed: 2183046]
39. Anderson JE, Ovalle WK, Bressler BH. Electron microscopic and autoradiographic characterization of hindlimb muscle regeneration in the mdx mouse. The Anatomical record. 1987; 219(3):243–257. [PubMed: 3425943]
40. McGeachie JK, Grounds MD, Partridge TA, Morgan JE. Age-related changes in replication of myogenic cells in mdx mice: quantitative autoradiographic studies. J Neurol Sci. 1993; 119(2): 169–179. [PubMed: 8277331]
41. Radley HG, Grounds MD. Cromolyn administration (to block mast cell degranulation) reduces necrosis of dystrophic muscle in mdx mice. Neurobiology of disease. 2006; 23(2):387–397. [PubMed: 16798005]
42. Shavlakadze T, White J, Hoh JF, Rosenthal N, Grounds MD. Targeted expression of insulin-like growth factor-I reduces early myofiber necrosis in dystrophic mdx mice. Molecular therapy: the journal of the American Society of Gene Therapy. 2004; 10(5):829–843. [PubMed: 15509501]
43. Passaquin AC, Renard M, Kay L, Challet C, Mokhtarian A, Wallimann T, Ruegg UT. Creatine supplementation reduces skeletal muscle degeneration and enhances mitochondrial function in mdx mice. Neuromuscular Disorders. 2002; 12(2):174–182. [PubMed: 11738360]
44. Khurana TS, Watkins SC, Chafey P, Chelly J, Tome FM, Fardeau M, Kaplan JC, Kunkel LM. Immunolocalization and developmental expression of dystrophin related protein in skeletal muscle. Neuromuscular disorders: NMD. 1991; 1(3):185–194. [PubMed: 1822793]
45. Yokota T, Lu QL, Morgan JE, Davies KE, Fisher R, Takeda S, Partridge TA. Expansion of revertant fibers in dystrophic mdx muscles reflects activity of muscle precursor cells and serves as an index of muscle regeneration. Journal of cell science. 2006; 119(Pt 13):2679–2687. [PubMed: 16757519]
46. Vilquin JT, Brussee V, Asselin I, Kinoshita I, Gingras M, Tremblay JP. Evidence of mdx mouse skeletal muscle fragility in vivo by eccentric running exercise. Muscle Nerve. 1998; 21(5):567–576. [PubMed: 9572235]
47. Wooddell CI, Zhang G, Griffin JB, Hegge JO, Huss T, Wolff JA. Use of Evans blue dye to compare limb muscles in exercised young and old mdx mice. Muscle Nerve. 2010; 41(4):487–499. [PubMed: 19813196]
48. Keeling RM, Golumbek PT, Streif EM, Connolly AM. Weekly oral prednisolone improves survival and strength in male mdx mice. Muscle Nerve. 2007; 35(1):43–48. [PubMed: 16969833]
49. Lefaucheur JP, Pastoret C, Sebille A. PHENOTYPE OF DYSTROPHINOPATHY IN OLD MDX MICE. Anatomical Record. 1995; 242(1):70–76. [PubMed: 7604983]
50. Bun SS, Kober F, Jacquier A, Espinosa L, Kalifa J, Bonzi MF, Kopp F, Lalevee N, Zaffran S, Deharo JC, Cozzone PJ, Bernard M. Value of in vivo T2 measurement for myocardial fibrosis

assessment in diabetic mice at 11. 75 T. Investigative radiology. 2012; 47(5):319–323. [PubMed: 22488510]

51. Anderson SW, Jara H, Ozonoff A, O'Brien M, Hamilton JA, Soto JA. Effect of disease progression on liver apparent diffusion coefficient and T2 values in a murine model of hepatic fibrosis at 11. 7 Tesla. MRI Journal of magnetic resonance imaging: JMRI. 2012; 35(1):140–146. [PubMed: 21990020]
52. Scalera JE, Soto JA, Jara H, Ozonoff A, O'Brien M, Anderson SW. Multiexponential T(2) analyses in a murine model of hepatic fibrosis at 11. 7 T. MRI NMR in biomedicine. 2013; 26(1): 83–90. [PubMed: 22674663]
53. Ebdrup S, Refsgaard HH, Fledelius C, Jacobsen P. Synthesis and structure-activity relationship for a novel class of potent and selective carbamate-based inhibitors of hormone selective lipase with acute in vivo antilipolytic effects. Journal of medicinal chemistry. 2007; 50(22):5449–5456. [PubMed: 17918819]
54. Ababneh Z, Beloeil H, Berde CB, Gambarota G, Maier SE, Mulkern RV. Biexponential parameterization of diffusion and T2 relaxation decay curves in a rat muscle edema model: decay curve components and water compartments. Magnetic resonance in medicine: official journal of the Society of Magnetic Resonance in Medicine/Society of Magnetic Resonance in Medicine. 2005; 54(3):524–531.
55. Cole WC, LeBlanc AD, Jhingran SG. The origin of biexponential T2 relaxation in muscle water. Magnetic resonance in medicine: official journal of the Society of Magnetic Resonance in Medicine/Society of Magnetic Resonance in Medicine. 1993; 29(1):19–24.
56. Saab G, Thompson RT, Marsh GD. Effects of exercise on muscle transverse relaxation determined by MR imaging and in vivo relaxometry. Journal of applied physiology (Bethesda, Md: 1985). 2000; 88(1):226–233.
57. Heemskerk AM, Drost MR, van Bochove GS, van Oosterhout MF, Nicolay K, Strijkers GJ. DTI-based assessment of ischemia-reperfusion in mouse skeletal muscle. Magnetic resonance in medicine: official journal of the Society of Magnetic Resonance in Medicine/Society of Magnetic Resonance in Medicine. 2006; 56(2):272–281.

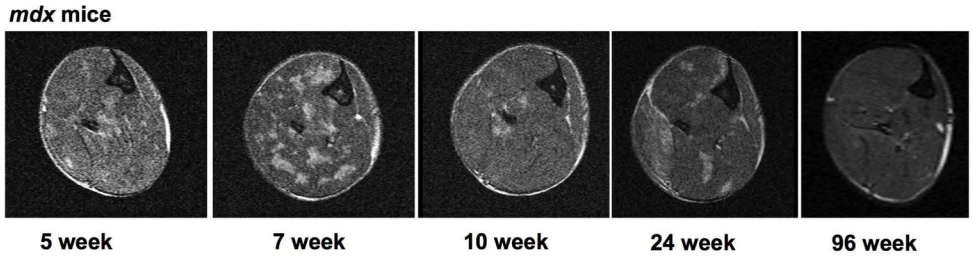

Figure 1.

Representative transaxial T_2 weighted images of lower hindlimb muscles at the mid-belly region of *mdx* mice across time points.

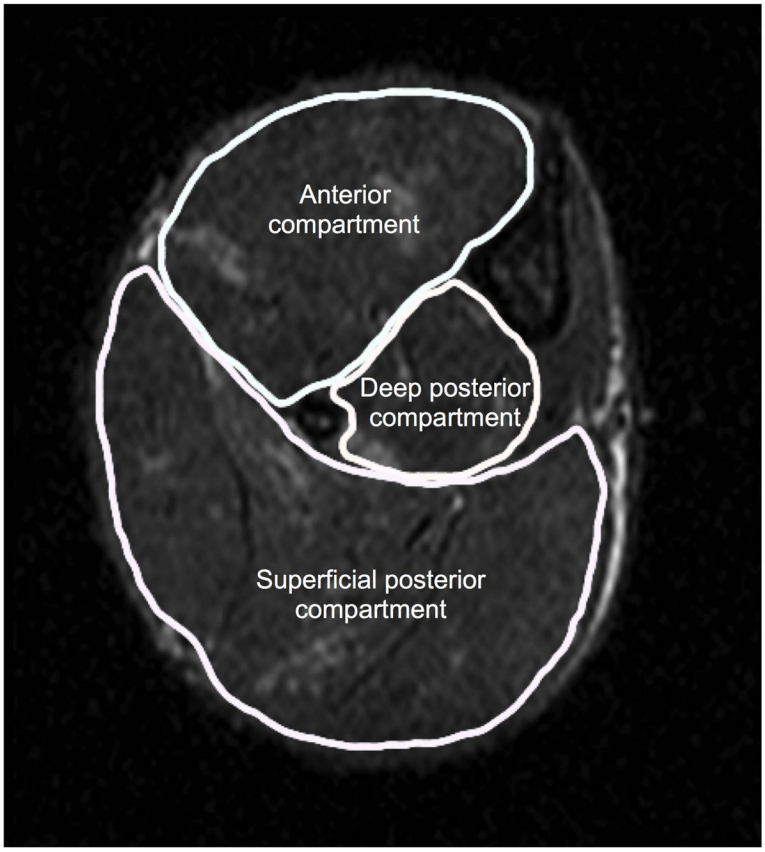

Figure 2.
Transaxial MR image taken at the mid-belly region of *mdx* lower hindlimb showing anterior and posterior compartments for muscle T_2 analysis. The anterior compartment includes tibilais anterior and extensor digitorum longus; the posterior compartment includes gastrocnemius, soleus, and plantaris.

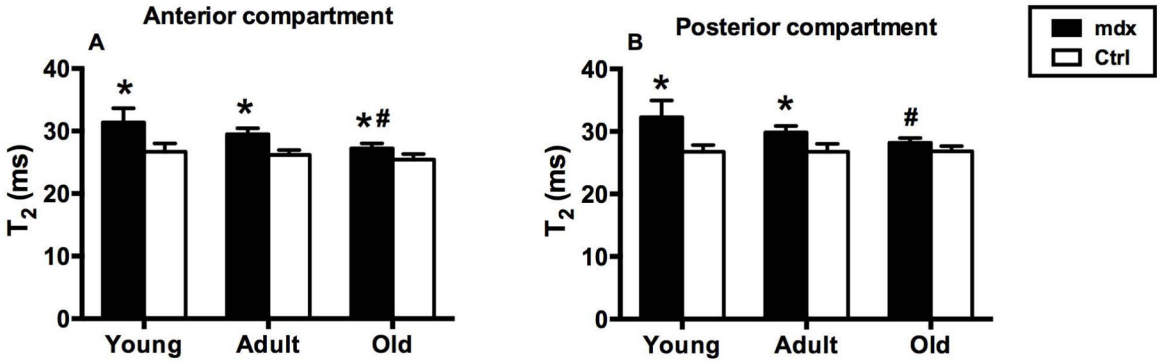

Figure 3.

Muscle T_2 values in (A) anterior and (B) posterior compartments in young (5 – 24 weeks), adult (44 weeks), and old *mdx* (96 weeks) and control mice. **(A)** In anterior compartment, the *mdx* mice had higher T_2 values in all age groups than control mice (* $P<0.05$). T_2 values in old *mdx* mice were significantly lower than young and adult *mdx* mice. ($^{\#}$ $P<0.05$). **(B)** In posterior compartment, the *mdx* mice had higher T_2 values in young and adult groups than age-matched controls (*$P<0.05$). T_2 values of old *mdx* mice were significantly lower than young and adult *mdx* mice.

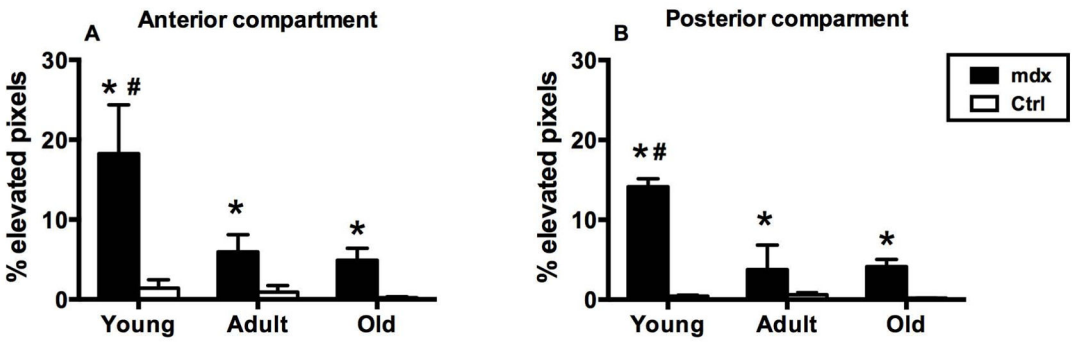

Figure 4.

Percent elevated pixels in **(A)** anterior and **(B)** posterior compartments in young, adult, and old *mdx* and control mice. In anterior and posterior compartments, the *mdx* mice had higher T_2 values in all age groups than control mice (* $P<0.05$). Young *mdx* mice had significantly higher % elevated pixels than adult and old *mdx* mice. ($^{\#}$ $P<0.05$).

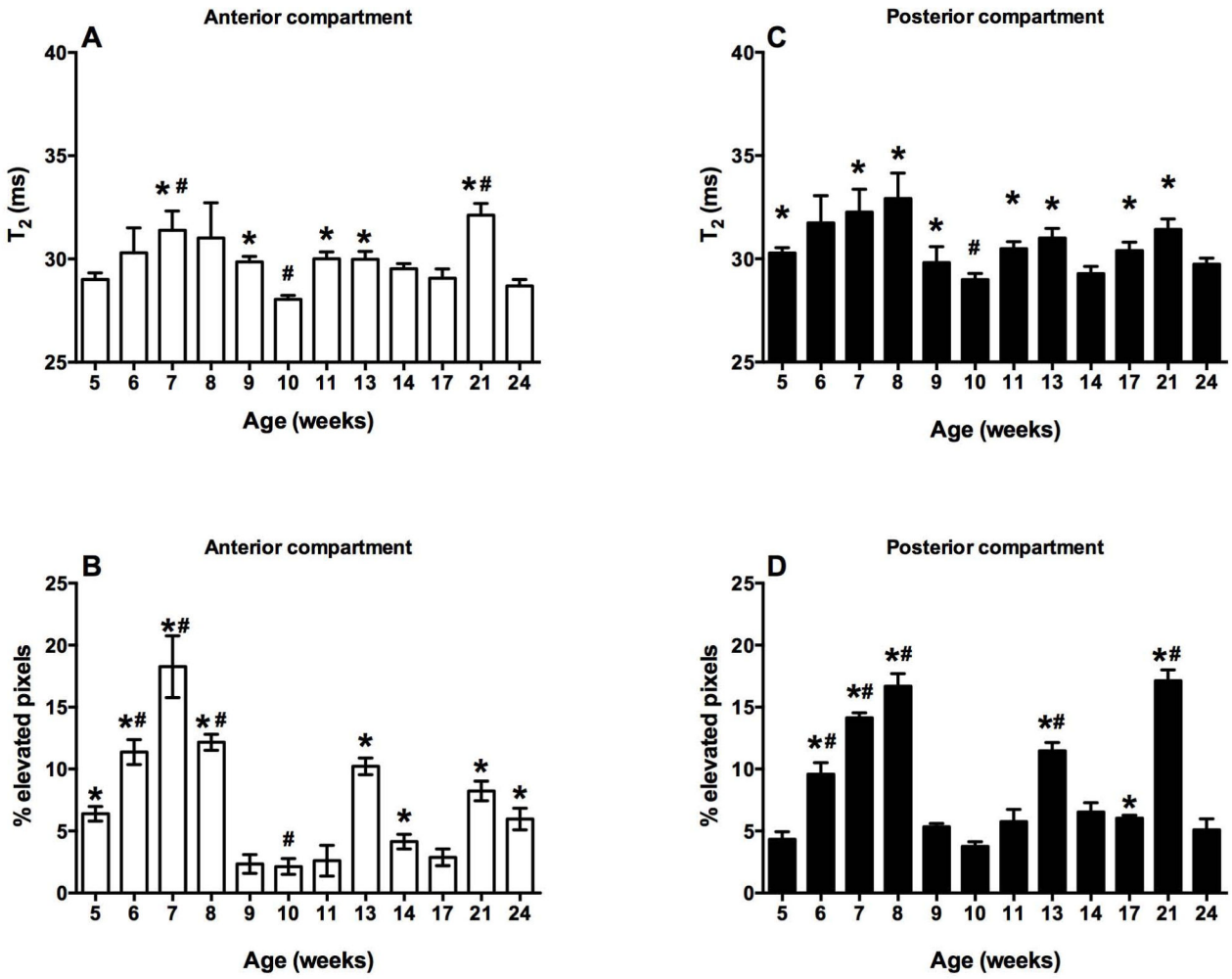

Figure 5.

Mean muscle T_2 and % pixels with elevated T_2 in anterior **(A, B)** and posterior **(C, D)** compartments of *mdx* mice (mean ± SEM). Mean T_2 and % pixels with elevated T_2 of anterior and posterior compartment are highest between 7–8 weeks and lowest at 10-weeks. * represents significant difference from 10 week time point ($P<0.05$) and # represents significant difference from 5 week time point ($P<0.05$).

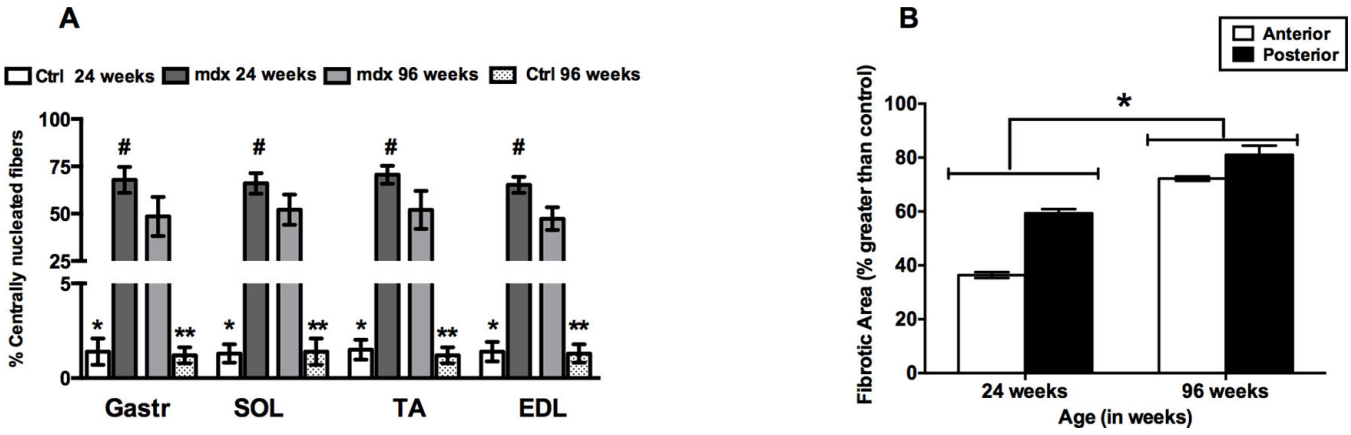

Figure 6.

(A) Quantification of CNF of *mdx* and age-matched Ctrl mice. * represents significant difference between Ctrl and *mdx* mice at age 24 weeks, ** represents significant difference between Ctrl and *mdx* mice at age 96 weeks, # represents significant difference between young and old *mdx* mice ($P<0.05$). **(B)** Quantification of percent fibrotic/necrotic tissue in the hindlimb muscles of *mdx* mice at 24 and 96 weeks. Significant difference was found between hindlimb muscles of *mdx* mice at the 24- and 96-week time points (* $P<0.05$).